HAL
open science

The roles of hydration and evaporation during the drying of a cement paste by localized NMR

Maxime van Landeghem, Jean-Baptiste d'Espinose, Bernhard Blümich, Jean-Pierre Korb, Bruno Bresson

To cite this version:

Maxime van Landeghem, Jean-Baptiste d'Espinose, Bernhard Blümich, Jean-Pierre Korb, Bruno Bresson. The roles of hydration and evaporation during the drying of a cement paste by localized NMR. Cement and Concrete Research, 2013, 48, pp.86 - 96. 10.1016/j.cemconres.2013.01.012 . hal-01537697

HAL Id: hal-01537697

https://hal.sorbonne-universite.fr/hal-01537697v1

Submitted on 20 Jan 2021

HAL is a multi-disciplinary open access archive for the deposit and dissemination of scientific research documents, whether they are published or not. The documents may come from teaching and research institutions in France or abroad, or from public or private research centers.

L'archive ouverte pluridisciplinaire **HAL**, est destinée au dépôt et à la diffusion de documents scientifiques de niveau recherche, publiés ou non, émanant des établissements d'enseignement et de recherche français ou étrangers, des laboratoires publics ou privés.

The roles of hydration and evaporation during the drying of a cement paste by localized NMR

Maxime Van Landeghem [a,b,c], Jean-Baptiste d'Espinose de Lacaillerie [a], Bernhard Blümich [b], Jean-Pierre Korb [d], Bruno Bresson [a,*]

[a] Sciences et Ingénierie de la Matière Molle, UMR 7615 CNRS UPMC, ESPCI ParisTech, 10 rue Vauquelin, 75005 Paris, France
[b] ITMC, RWTH-Aachen Worringer Weg 1, D52056 Aachen, Germany
[c] Saint-Gobain Recherche, 39 quai Lucien Lefranc, BP 135, 93303 Aubervilliers cedex, France
[d] Physique de la Matière Condensée, Ecole Polytechnique, CNRS, 91128 Palaiseau, France

ARTICLE INFO

Article history:
Received 25 July 2012
Accepted 29 January 2013

Keywords:
Drying (A)
Pore Size Distribution (B)
Transport Properties (C)
Humidity (A)
Hydration (A)

ABSTRACT

The moisture distribution during the setting of a thin mortar layer can be particularly complex to manage under dry (20% RH) and hot weather (above 25 °C) conditions. To better understand the fundamental phenomena at stake, we used static gradient relaxation NMR tools such as Profile MOUSE and STRAFI. This allowed disentangling the mutual effect of evaporation and self-desiccation by hydration. The interest of combining the two techniques is that the capillary water is observed with the MOUSE while STRAFI reveals quantitatively the build-up of the hydrate gel nanostructure. Spatially resolved and 2D relaxation exchange experiments on a model white cement paste revealed that although evaporation induced a capillary water gradient, the kinetics of the building of the pore structure and its homogeneity remained unaffected.
© 2013 Published by Elsevier Ltd.

1. Introduction

The knowledge of the moisture distribution in building materials and more generally the transport properties of the adsorbed water phase are a key-point for the understanding of their durability. Drying can induce cracking and is a matter of permanent concern for the mortar and concrete industry. At a smaller scale, the mechanical resistance of cementitious materials is linked to the density of the C–S–H phase which is largely determined by the relative volume of the water saturated C–S–H gel nanopores. The physics of drying has been described with great success both at the theoretical [1] and experimental [2] levels for model porous systems. However a cement paste represents a more complex challenge as the pore volume cannot be considered constant and water is a chemically reactive phase.

When a Portland cement powder is mixed with water, a chemical hydration reaction occurs [3]. The soluble components present in the cement powder, when in contact with water, dissolve quickly, creating a saturated solution from which the hydrates precipitate. The hydrates grow on the surface of the cement grain, connecting the grains to each other and hardening the then solid material. Cement-paste hardening is thus intrinsically accompanied by a liquid water consumption called self-desiccation. Self-desiccation corresponds to the transformation of part of the liquid water into solid hydrates. It must be distinguished from true drying which corresponds to the removal of liquid water by transfer to the gas phase, that is evaporation at the paste/air interface. The matter is further complicated by the possible interplay between self-desiccation and evaporation: the tortuous hydrate network affects the water transport toward the interface for evaporation, while one can expect, in turn, that evaporation, by decreasing the local water/cement ratio, affects the formation of the hydrate network. In the following, we will refer to the simultaneous effects of evaporation and self-desiccation as “drying”.

The ultimate aim of our study is to assess during drying the mutual roles of evaporation and self-desiccation on the final porous structure. In that respect, the state and the distribution of water molecules within the cement paste is fundamental for the understanding of its evolving pore structure, and Nuclear Magnetic Resonance (NMR) is one of the few non invasive methods that can deliver this information. Indeed, it is now well established that proton NMR relaxation-rate measurements (both spin–spin relaxation referred to as T_2 relaxation and spin–lattice relaxation referred to as T_1 relaxation) give access not only to the water content but also to the saturated pore-size distribution of a hydrating cement paste.

For all kinds of cement, it is now accepted that the paramagnetic impurities at the surface of the pores control the NMR relaxation rate of all the water protons in the pore, even for white cement (with low concentration of Fe). The relaxation process is the following: the

water molecules undergo a 3D diffusion in the pore, and, at some point, a water molecule reaches the surface of the pore where its diffusion is restricted, before returning to the bulk of the pore [4]. During its stay on the surface, the water molecule can enter the vicinity of a paramagnetic impurity embedded within the pore wall. The magnetic interaction with the paramagnetic centers is then the dominant contribution to the relaxation, even for cement with low Fe content.

Since the surface residence time is very short compared to the NMR measurement time (fast exchange limit), the effective relaxation rate $(T_2^{\mathrm{eff}})^{-1}$ of water is an average of the bulk liquid relaxation rate $(T_2^{\mathrm{bulk}})^{-1}$ and the enhanced surface relaxation rate, weighted according to the surface-to-volume ratio S/V of the pore [5]:

$$\frac{1}{T_2^{\mathrm{eff}}} = \frac{1}{T_2^{\mathrm{bulk}}} + \rho\frac{S}{V} \tag{1}$$

where ρ is the surface relaxivity. Thus, the relaxation rate reflects the pore size and morphology.

For the complete pore network, the total experimental magnetic decay $S(t)$ is the superposition of the exponential decays T_2^{effi} characteristic of each pore size weighted by their relative population A_i:

$$S(t) = \sum_n A_i \exp\left(-\frac{t}{T_2^{\mathrm{effi}}}\right). \tag{2}$$

Therefore, in principle, NMR relaxation analysis can provide the relative abundance of each water population in the cement paste (in the hydrate structure, in the C–S–H gel pores, and in the capillary pores) and can even provide the corresponding pore size distribution [6]. The problem is thus to recover the pore size distribution from the time relaxation of the NMR signal. The corresponding mathematical procedure is formally a Laplace inversion. This operation, a key-point of the analysis, was recently facilitated by the availability of stable multi-dimensional algorithms executable on desktop computers [7].

In a typical white cement paste hydrated during a few days with a water/solid ratio of 0.4, the extraction of each T_2^{effi} component of the relaxation leads to a discrete distribution which ranges from 10 μs up to 1 s [8]. Numerous NMR experiments carried out at different frequencies (from kHz up to MHz) have led to the following conclusions: all the water molecules in a hydrated cement paste can be categorized as belonging to different relaxation components. The first component is fast relaxing with T_2^{eff}s of 15 μs [9]. It corresponds to the hydroxyl group in the Portlandite. The second component with T_2^{eff} between 100 μs and 400 μs corresponds to the water associated to the hydrate nanostructure. In this category, the structural water of the C–S–H interlayer and the water contained in the nanopores of the C–S–H gel were included. Indeed, the C–S–H is inherently nanoporous, and although the water contained in those very small pores (2 nm) is not chemically speaking structural, its removal would imply the development of extreme capillary pressures that would destroy the gel nanostructure as well. Another T_2^{eff} component of the cement paste proton NMR signal ranges from about 1 ms to 200 ms. It arises from water in pores scaling from a few nanometers up to less than a micrometer and is called the capillary water. The specificity of this type of water is that it can be reversibly removed without any destruction of the nanostructure of the cement paste. Finally, a last component of slowly relaxing protons (circa 1 s) corresponds to free liquid-like water. It must be noted upfront that in presence of a gradient, this population cannot be distinguished as its T_2^{eff} is compressed by diffusive effects toward the range of T_2's capillary water. In this study, we placed a cut-off at T_2^{eff} equal to 150 μs which means that all the water moistures with a T_2^{eff} below 150 μs are included in the same component (hydroxyl groups and gel water). Table 1 summarizes the T_2^{eff} values that were actually accessible in our study.

Table 1
T_2^{eff} values actually accessible versus pore size and proton populations.

T_2^{eff} range	Pore size according to [8]	Proton population
Above 150 μs	2 nm	"Gel" water
1 ms to 200 ms	(1 ms) 16 nm (50 ms) 170 nm (200 ms) 270 nm	Capillary water
1 s		Free water

The same conclusions can be essentially drawn from T_1 relaxation rates analysis. By T_2 analysis even without a predictive relaxation model, some authors [10] were able to draw precise conclusions about the evolution of each kind of water during the hydration cement paste.

To follow the drying, the simplest study can be performed on the bulk material. However, to actually discriminate drying and desiccation mechanisms, the monitoring of the total water in the sample versus time is not sufficient. Due to the anisotropy of the evaporation process, it is necessary to follow the distribution and evolution of water within the pore system not only in time but also in space. This justifies the combination of NMR relaxation with MRI (Magnetic Resonance Imaging) techniques. As all of the evaporation occurs at the paste/air interface, one-dimensional profiling methods are the most adequate tool. When dealing with a cement paste, the MRI technique must rely on stable and large gradient to overcome the rapid relaxation rates (see Table 1). This reduces the techniques of choice to the ones involving strong static gradients, such as STRAY Field Imaging (STRAFI). Indeed, there is already a significant body of literature concerning the study cement paste using the high stray fields of superconducting magnets [11–15], but never as a function of the temperature and humidity, which however influences deeply the drying. As a result, most studies have focused on self-desiccation and pore network built-up. Alternatively, some authors have chosen to use single sided permanent magnets with lower fields and static gradients such as the GarField [16] or the Profile NMR MOUSE [17].

The present study is thus by far not the first one to apply STRAFI or single-sided magnet methods to the setting of a cement paste but here we focus on the simultaneous effects of self-desiccation and evaporation by varying the temperature and humidity conditions. Furthermore, we combined the two complementary NMR profiling methods: NMR imaging in the Stray Field of the superconducting magnet (referred to as STRAFI experiment in the following) [14,18] and imaging by NMR-MObile Universal Surface Explorer (referred to as Profile MOUSE experiment in the following) [17]. The versatile Profile MOUSE experiment is a powerful tool to profile the water distribution in a cement paste at different temperature as it is portable and can easily fit into climate chambers. In a first part, the Profile MOUSE results are presented. They show the effect of drying on the upper face of the paste (the face in contact with air) and the effect of temperature on the water distribution as a function of the depth in the sample. The complete interpretation of the drying process needs the observation of all kinds of water in the cement (free water or water in the pore structure, gel water, as well as structural water in the hydrates). The STRAFI experiments carried out with a home-made NMR probe combine imaging (open geometry of the probe so that the sample can be moved through the coil) and solid state NMR advantages (short pulse, short dead time, short echo time). In a second part of the paper, the evolution of the porous network in a slice of the paste is presented. It is shown how bulk proton NMR relaxation experiments usually performed in a cement paste (T_1-T_2 correlation maps, T_1 and T_2 distribution) can be adapted to be spatially resolved. In a third part of the paper, the effect of relative humidity is studied independently of temperature. In the last part, the combined effect of temperature and relative humidity is addressed.

2. Materials and methods

The principle of the Profile MOUSE [19,17] and STRAFI [14,18] experiments has been described elsewhere and only the main features of the experiment are recalled.

2.1. Profile MOUSE setup for studies with humidity and temperature control

The Profile MOUSE used in this work is a unilateral NMR sensor which is specially designed to generate a magnetic field with a uniform gradient in a sensitive volume located at 25 mm over the surface of the magnet [19,17]. This allows 1D profiling over a range of 25 mm at a magnetic field of 0.32 T (^{1}H frequency of 13.8 MHz). The magnetic field gradient over the sensitive slice is 7.5 T/m. The magnet is mounted on a lift which allows its movement in relation to the sample. Due to the presence of a magnetic field gradient, when a finite radiofrequency pulse is emitted at the frequency of 13.8 MHz, only a thin slice (typically 100 μm) is excited. This thin slice is excited using a CPMG sequence in order to measure its apparent transverse relaxation rate $T_2^{\mathrm{app}-1}$ [20]. The apparent T_2^{app} for a species of diffusion coefficient D is related in presence of a gradient G to the T_2^{eff} through the following formula:

$$\frac{1}{T_2^{\mathrm{app}}} = \frac{1}{T_2^{\mathrm{eff}}} + D \cdot \frac{\gamma^2 G^2 t_E^2}{12} \tag{3}$$

where γ is the gyromagnetic ratio and t_E is echo time of the CPMG sequence. Hereafter, it must be understood that what is referred as T_2 is actually T_2^{app} in order to keep a compact notation.

The echo time was set to 140 μs. Once the signal arising from this slice is acquired, the lift moves the magnet in order to measure the next step of the profile. The Profile MOUSE mounted on its lift fits a $38 \times 38 \times 38$ cm^3 box and can easily be introduced in a commercial temperature and humidity cabinet (see Fig. 1). This cabinet (model LHU-113) was provided by ESPEC®.

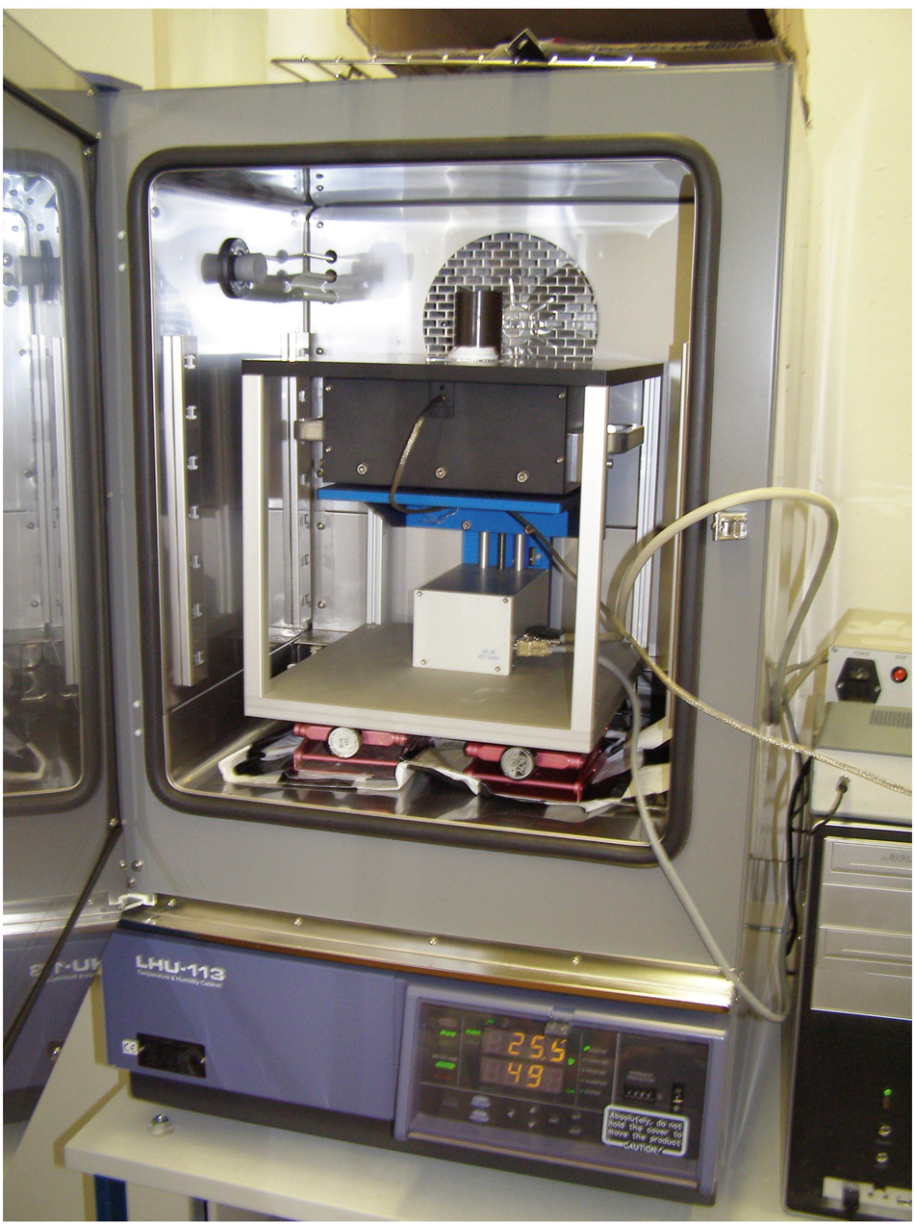

Fig. 1. Picture of the Profile MOUSE setup. It was operated inside a temperature and humidity cabinet. The sample sits at the top of the black plate. During profiling, the sensor is moved step by step from top to bottom relative to this plate so the whole profile can be scanned.

2.2. STRAFI setup

STRAFI can be seen as a high field version of the Profile MOUSE. In the STRAFI, the sample is placed out of the bore of the superconducting NMR magnet, along the magnet axis. It is then moved to a location where the static magnetic field fringe gradient from the superconducting magnet is homogeneous across a slice perpendicular to the axis of the magnet. As with the profile MOUSE, this slice is used for imaging. We recently reported [18] how to find this position in the fringe field and the way to align the sample with respect to the superconducting magnet so that a spatial resolution of 5 μm could be achieved on a sample with a lateral extension of 1 cm. From then on, the procedure to complete the profile of the sample is comparable to the one described for the Profile MOUSE, except that the sample is mobile and not the magnet. The sample is placed on top of a rod driven by a lift which repositions it between each NMR acquisition. Besides the high resolution which can be achieved with this setup, STRAFI exhibits another significant advantage arising from the high static gradient and the use of a solid-like imaging probe at high field (homemade): it allows access to very short T_2 values (typically hundreds of microsecond using CPMG detection train with echo times of the order of a few tens of μs). Indeed, the ring-down time decreases with increasing frequency. This means that it is possible to combine good spatial resolution, measurement of short T_2 values such as that of gel water in C–S–H and benefit from the high field detection. In fact, the magnetic field at which our STRAFI experiments were carried out on our Oxford 7 T magnet was 3.2 T, corresponding to a proton larmor frequency of 137 MHz. At this position, the value of the magnetic field gradient was about 52 T/m. This high static gradient (as well as the one of the Profile MOUSE) is the key to success for imaging rigid materials. Indeed, it is sufficiently large to overcome any loss of resolution arising in solids from magnetic susceptibility gradients and dipolar interactions [21].

The STRAFI probe was fitted by a humidity and temperature control custom-made setup (Fig. 2). The cement paste was poured in 30 mm tube. The thickness of the cement paste was 10 mm and the upper surface was in contact with air. The temperature was controlled by a commercial NMR temperature unit manufactured by Eurotherm®. A thermocouple placed close to the sample allowed the regulation of a heater inside a dewar positioned at the bottom of the probe. The temperature which could be maintained ranged between 20 °C (ambient temperature) and 80 °C. The humidity was regulated by manually mixing dry air with water saturated air drawn from a bubbler. This setup allowed humidity levels from 10 to 70% RH.

2.3. Preparation of the white cement paste

The white cement was provided by Saint-Gobain Recherche (white cement CEM II) and used as received. The cement paste was prepared with a water/cement ratio of 0.4. In the case of experiments using the Profile MOUSE, the paste was prepared in a conventional 250 mL container, directly placed on the plate above the sensor. For the STRAFI measurements, the water and cement pastes were cast into a 10 mm glass tube. The unsealed tube was then introduced into the glass cylinder of our homemade probe which is used to guide the sample and regulate humidity and temperature.

3. Results and discussion

3.1. Complementarity of the profile MOUSE and STRAFI

The determination of the pore structure of cement by proton NMR requires the measurement of the signal decay (see Eq. (2)). This measurement was performed using the CPMG sequence which consists of a 90° pulse followed by a train of 180° pulses [22,23]. Each echo was recorded independently. The first echo obtained was removed as its amplitude is determined by factors different from those of the other echoes [23]. The obtained decay was then either fitted by multi-exponential functions or inverted using the inverse Laplace transformation (ILT) algorithm. Besides the fine dependence of T_2 with the pore size (see Table 1), two T_2s (or distribution of T_2s) are usually expected in white cement paste in presence of a gradient. As stated in the introduction, this corresponds to water in capillary pores and structural water in the hydrates. Fig. 3 exhibits typical CPMG decays of a white cement paste obtained using the Profile MOUSE (a) and STRAFI (b). Both decays corresponded to a drying of 8 h. The associated ILT is exhibited in Fig. 3 (c and d), respectively. In the case of the Profile MOUSE, the distribution of T_2s seemed mono-modal. The single peak was attributed to capillary water. The echo time of the Profile MOUSE (140 μs) does not allow to see relaxing species with a T_2 shorter than a few hundreds of microseconds. Thus, "gel" water and structural water are naturally filtered out when white cement is measured with this tool. On the contrary, the T_2 distribution recorded by STRAFI was bimodal (see Fig. 3d). This could be achieved because the echo time in the CPMG detection is much shorter (40 μs). The two peaks are attributed to capillary water (T_2 around 1 ms) and "gel" water (T_2 around 100 μs). Still the chemically structural water (T_2 expected around 10 μs) cannot be seen by STRAFI. As a consequence, this preliminary study shows that the two tools complement each other. The Profile MOUSE being sensitive to long T_2s is a simple indicator for change in capillary water content within white cement due to transfer to the interface such as during evaporation. The STRAFI being sensitive also to "gel" water is expected to provide more information about the pore structure.

3.2. Evolution of the pore structure of white cement

3.2.1. 1D experiment

To follow the evolution of the porous structure of white cement, a sample of white cement paste was prepared and measured by STRAFI using a CPMG detection train. This measurement was performed at a depth of 10 mm from the surface of the sample in order to accumulate more scans and obtain the better signal-to-noise ratio necessary for a good ILT. The experiment lasted one day, and one decay was measured every 17 min. Afterwards, each decay was numerically inverted to provide the T_2 distribution versus the hydration time (Fig. 4a) while a double exponential fit was also performed. The amplitudes of the two decays are displayed in Fig. 4b. During the first 4 h of hydration, a single T_2 could be realistically defined with a good level of confidence and the distribution could be considered to be mono-modal, going from a T_2 of 4.5 ms at time $t = 0$, to 2 ms at $t =$ 5 h. Then a shorter T_2 population appeared after a hydration time of 10 h, while the amplitude of the population with the long T_2 decreased below the amplitude of the population with a short T_2. This corresponded to the setting time of the paste and the formation of the percolating C–S–H gel network. The long T_2 value shortened progressively from 1 ms down to 400 μs between 10 h and 20 h while the shorter T_2 was constant at about 150 μs.

Previous work [8] helped us to clearly attribute each kind of water to details of the pore structure. For example, $T_2 = 5$ ms observed at a drying time of about 6 h can be attributed to capillary pores of radius $r = 100$ nm, and $T_2 = 1$ ms has previously been attributed to pores of radius $r = 15$ nm. The short T_2 of 150 μs corresponds to the gel C–S–H nanopores of a few nanometers in diameter. However, the T_2 of the chemically bound water (10–30 μs) [12] (C–H and chemically structural water of C–S–H) was not observed in the previous analysis. Actually, it must be recalled that the first echo of the CPMG train was removed as it is known to be weighted by a factor 2/3 in the presence of a magnetic field gradient [20,23]. However, we noticed that the first echo occurring 30 μs after the first pulse was much more intense than the others. This could be interpreted as the contribution of the

Fig. 2. Picture of the STRAFI setup. The sample is placed just outside the bore of the superconducting magnet at the top of an alumina rod driven by a stepper motor. Both humidity and temperature are regulated.

chemically bound water in cement hydrates which would have not completely relaxed yet. In order to stabilize the analysis, we nevertheless stuck to our choice of removing the first point before processing the data on Fig. 4 as well as in the following analysis.

The advantage of the experiment presented here is the clear attribution of the different kinds of water which successively appear in the material. It also evidences the discrete characteristic of the pore network developing with the time. The interesting result is that it can be performed with spatial resolution. An example of this kind of analysis is depicted in Fig. 5. Fig. 5a exhibits profiles of white cement measured at various hydration times using only the first echo of the CPMG echo train. At 25 °C and 30%RH a clear variation of the water distribution is observed along the sample. To check if drying affects or not the kinetics of structuring of the material, a T_2 analysis similar to the one of Fig. 4b was performed at various heights in the sample: at the surface of the sample, at a depth of 3 mm from the surface and at a depth of 10 mm. The kinetics of emergence of the population with the short T_2 (red curve) as well as that of the decrease of the population with long T_2 at these positions (Fig. 5b, c, and d) were virtually identical at this position. This showed that the kinetics of the structuring was not affected by the drying.

3.2.2. 2D experiment

The previous 1D studies performed by STRAFI at a single height can be completed by 2D T_1-T_2 NMR experiments which can be adapted for use in inhomogeneous magnetic field [24], and some applications to the study of cement pastes have been reported [16,25]. The sequence we used was a saturation recovery sequence [26] followed by a mixing time τ varying logarithmically [22] and a CPMG detection train.

A T_1-T_2 2D NMR experiment was carried at a fixed position, in the middle of the paste. The 2D data were processed by 2D inverse Laplace transformation adapted to the study of T_1-T_2 correlations [27]. Fig. 6 displays the T_1-T_2 maps of a white cement paste (w/c = 0.4) for two hydration times. After 6 h of hydration (Fig. 6a), the 2D correlation map of the white cement exhibited a single peak at (T_1 = 15 ms and

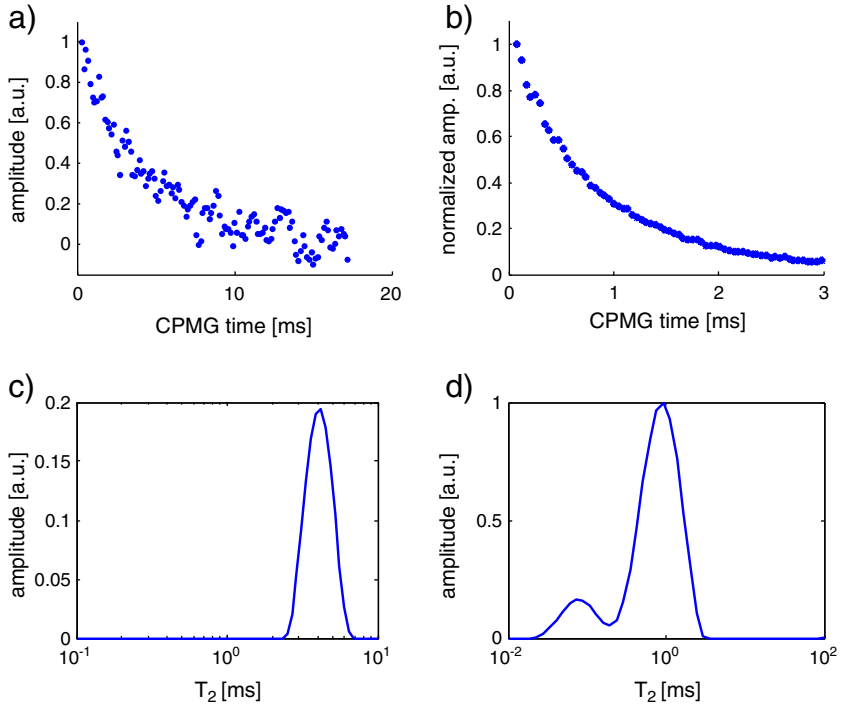

Fig. 3. CPMG decays and associated T_2 distributions of white cement prepared with a ratio water/cement of 0.4 after 8 h of drying. a) CPMG decay obtained using the Profile MOUSE. The echo time was set to 140 μs and the number of echoes to 128. The repetition time was 1 s and the number of scans 128. This led to an experimental time of about 2 min. b) CPMG decay obtained using STRAFI. The echo time was 40 μs and the number of echoes 400. Only the first 64 echoes are displayed. The repetition time was 1 s and the number of scans 1024, leading to a total experimental time of 17 min. c) T_2 distribution obtained from the ILT of the CPMG decay displayed in a). d) T_2 distribution obtained from the ILT of the CPMG decay displayed in b).

$T_2 = 4$ ms). Thus, at this time, the pore network appeared to be a completely percolated continuous phase. At time 4 days (Fig. 6b), a peak around $T_1 = 2-3$ ms and $T_2 = 400$ μs appeared along with a peak at $T_1 = 800$ μs and $T_2 = 150$ μs. The first noticeable result was that the peaks stay on the line $T_1 = 5T_2$, demonstrating that the behavior of the water molecules followed the theory briefly sketched in the introduction [8]. Indeed, one of the consequences of this theory is the dependence of the ratio T_1/T_2 on a few set of predictable parameters (namely the surface hoping time and the residence time on the surface of the pore). The second remark is that on the time scale of the experiment, no exchange peak was observed for 4-day hydration. Thus the two porous networks observed at that stage were almost disconnected. The third remark is that according to the literature [8], the difference between the correlation map shown in Fig. 6a and b could be interpreted in the following way: the disappearance of the peak at $T_1 = 15$ ms and $T_2 = 2.5$ ms was due to the conversion of the capillary water in large pores into capillary water in smaller pores of $T_1 = 2$ ms and $T_2 = 400$ μs and into C–S–H "gel" water of $T_1 = 800$ μs and $T_2 = 150$ μs. The C–S–H gel had then significantly evolved. This interpretation supports the discrete interpretation of the pore structure.

3.2.3. Conclusion of the STRAFI experiments

The experiments complement each other and global conclusions can be drawn. First of all, from Figs. 4a and 6b, it appeared that the relaxation time $T_2 = 150$ μs was invariant. The exchange with the network was weak. Indeed, if we attribute this T_2 to the 2 nm pore, called gel water, then, the amplitude of this T_2 component is simply a function of the amount of C–S–H in the paste and its position is

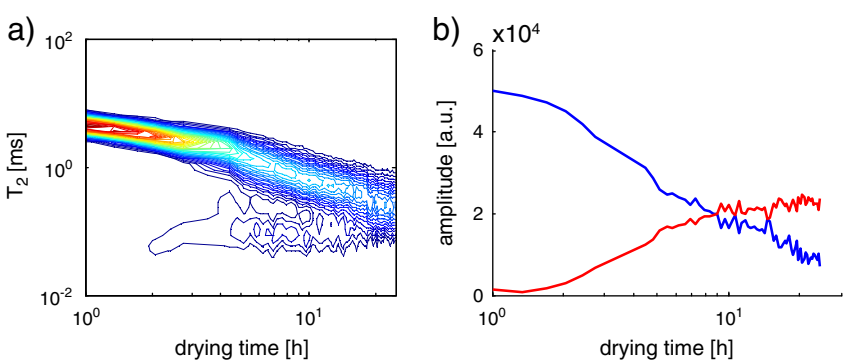

Fig. 4. a) T_2 distribution of a white cement prepared with a water/cement ratio of 0.4. This distribution is the result of a numerical ILT of CPMG decays measured by STRAFI at a depth of 10 mm within the sample. The CPMG train contains 400 echoes and the echo time is 40 μs. Using a recycle delay of 1 s and 1024 scans, one point was measured every 17 min. The color code reveals the intensity of each peak in the Laplace distribution. The red color corresponds to higher intensities in arbitrary units. b) Amplitude of the two populations evidenced by the ILT in a). This amplitude was obtained by double exponential fitting of the CPMG decay. The blue (resp. red) curve represents the population with long (resp. short) T_2.

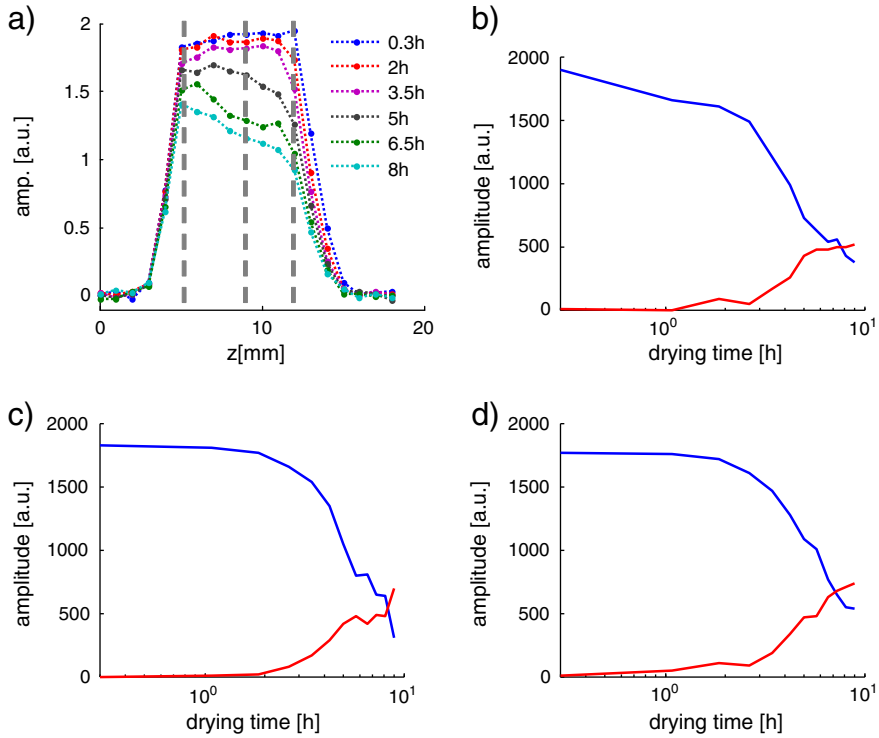

Fig. 5. a) STRAFI profiles measured at various hydration times following the preparation of a sample of white cement (w/c = 0.4) at 25 °C and 30% RH, using a CPMG detection train with an echo time of 40 μs. For the profiles, only the first echo was processed. The recycle delay was 1 s and the number of scans is 64 in order to complete the 19 points of the profile in 20 min. The vertical gray dotted lines correspond to the position where double exponential fits were performed. The corresponding amplitudes of the long T_2 (blue solid line) and short T_2 (red solid line) versus the hydration time are exhibited in plots (b) z = 5 mm, (c) z = 9 mm, and (d) z = 12 mm.

constant because the *S*/*V* ratio of the gel is fixed. Despite the fact that this water is part of a pore, the size of the pore does not change dramatically in the C–S–H. Moreover, this T_2 component appeared late in the hydration process. Considering the experiment from Fig. 4, it appears that the long T_2 value was decreasing continuously from $T_2 = 4$ ms down to $T_2 = 400$ μs. The evolution of the T_2 value with time (Fig. 4) and the evolution of the $T_1 - T_2$ correlation maps (Fig. 6) yielded very similar results. These values are also the same as those found by Holly et al. [29] on a white cement hydrated with a w/s ratio of 0.42. Besides getting access to the dynamics of the formation of the pore structure of white cement through the observation of the water distributions at a single position, STRAFI allows us to perform the same kind of study throughout the sample. Here, we showed for example (see Fig. 5) that the kinetics of the building of the pore structure of white cement was constant throughout the sample, even through evaporation induced a water gradient in the sample.

3.3. The effect of temperature investigated with the Profile MOUSE

Fig. 7 displays the NMR profiles obtained under 60% relative humidity at different hydration times and temperatures for a white cement paste. The sample was 22 mm thick and evaporation was allowed

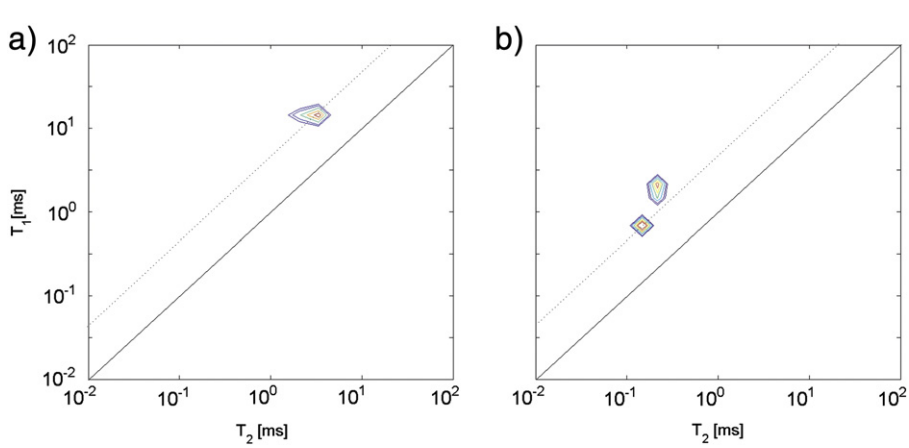

Fig. 6. 2D $T_1 - T_2$ NMR experiment performed by STRAFI at a depth of 3 mm from the surface in a sample of white cement (w/c = 0.4). The hydration time was (a) 6 h and (b) 4 days. The NMR sequence was a saturation recovery sequence (T_1 encoding) followed by a CPMG detection with a mixing time τ. The CPMG train consisted of 200 echoes with an echo time of 34 μs. The mixing time was set to vary logarithmically from 10 μs to 30 ms in 20 steps. Using a recycling delay of 1 s and 256 scans for each τ increment, the time to measure the full 2D map was close to 1 h.

only on the upper face of the sample at the position $z = 22$ mm. Two types of behavior could be distinguished depending on temperature. Below 25 °C, the profiles remained essentially flat except for a small region at the air interface of a few millimeters which is getting progressively dryer. The boundary of this region defines an evaporation front which progressed inward as drying proceeded. Above 25 °C, the behavior was the same during the first hours. However, behind the evaporation front, the profiles appeared progressively more tilted toward the air interface. To interpret theses data, it is important to recall that the Profile MOUSE setup is only sensitive to T_2s larger than 500 μs. As shown in Fig. 3, this means that in a cement paste, the Profile MOUSE detects only the capillary water. From these considerations, we can conclude that below 20 °C, the amount of free water remained homogeneously distributed behind the evaporation front during hydration and drying except within a millimeter of the air interface where the capillary pores appeared totally desaturated. These observations were consistent with the results already observed by Bohris et al. [12] and are interpreted as follows: desiccation by evaporation was very effective next to the air interface where there is almost no capillary water. On the other hand, in the bulk of the sample, the amount of capillary water decreased due to drying and self-desiccation but remains homogeneously distributed. The cement pore network efficiently redistributed the capillary water by capillary forces throughout the sample despite the unilateral evaporation. Behind the drying front, the drying mechanism is thus consistent with a funicular regime [28].

Above 25 °C, the situation appeared significantly altered. Although a funicular drying mechanism can still be postulated at the beginning, after a certain time (4 h for instance at 35 °C), the amount of capillary water varied across the depth of the paste. At these temperatures, the pore network in the paste does not allow a timely capillary water transfer. We suggest that the drying mechanism changed to a pendular regime [28] around 25 °C. Indeed, the effect of temperature can be either to induce a more efficient evaporation, or to speed up the hydration which prevents the capillary water transfer.

Fig. 8a and b exhibits the evolution of the amplitude and T_2 at various temperatures measured with the Profile MOUSE with respect to the hydration time of a white cement paste. The temperature affected drastically the kinetics of the setting of the cement paste. If one defines the setting as the inflection point of the curve amplitude versus drying time (Fig. 8a), we can see that it occurred at a drying time of about 20 h at 5 °C whereas it occurred at about 5 h at 35 °C. This result was consistent with the literature [30]. This evolution could also be seen in the change of T_2 with the drying time (Fig. 8b). Indeed, it exhibited a similar behavior. However, one can notice that the temperature affected not only the kinetics but also the values of T_2s. Fig. 8d shows a linear dependence of $1/T_2$ measured at the initial drying time as a function of temperature. This is interpreted as an effect of the temperature on the diffusion coefficient of water. Indeed, in a CPMG sequence performed in presence of a uniform magnetic field gradient G, the apparent T_2 is a function of the diffusion coefficient tD [31] which is a process activated with temperature (Eq. (3)).

When T_2 (Fig. 8b) is plotted as a function of the amplitude (Fig. 8a), one can see that all curves collapse to a single one (Fig. 8c) for all temperatures between 5 °C and 35 °C. The analysis of this master curve shows that it follows a power law with an exponent of 3. This is interpreted in the following way: According to Eq. (1), the effective T_2 in a porous medium is a function of the ratio S/V which is proportional to the pore size r in spherical geometries. As far as the amplitude is concerned, it is proportional to the amount of spins in capillary pores. This amount depends of the pore volume and varies as r^3 in the case of

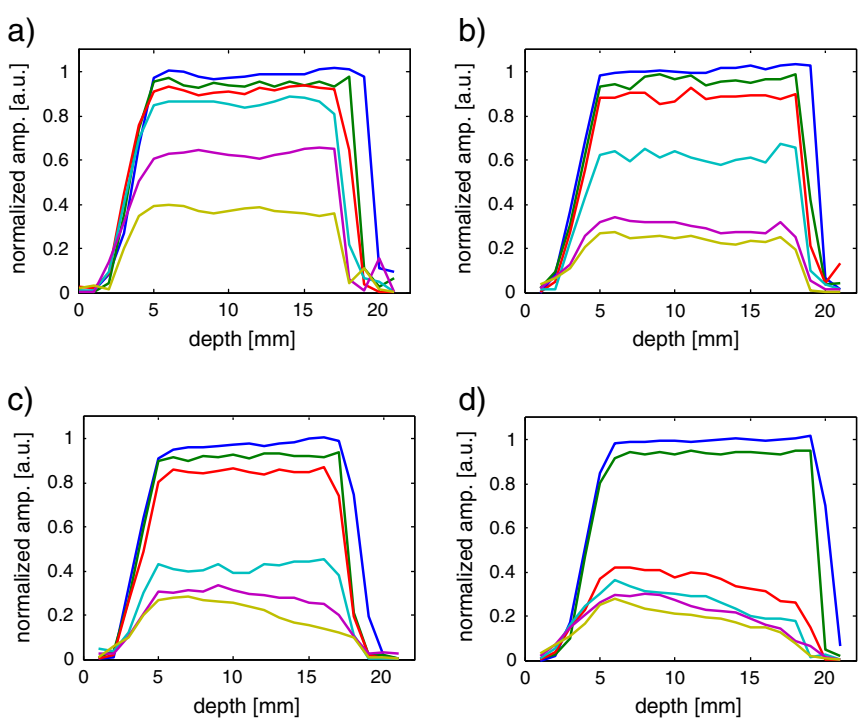

Fig. 7. Profiles obtained using the Profile MOUSE at various hydration times and temperatures: (a) 5 °C, (b) 20 °C, (c) 25 °C and (d) 35 °C on a white cement paste hydrated with a w/c ratio of 0.4. The profiles were measured over a range of 22 mm with a step size of 1 mm. For each temperature, a profile was measured at exponentially spaced intervals of time: 1 h, 2 h, 4 h, 8 h, 16 h and 32 h, corresponding to the 6 solid lines of each plot. For each point of the profile, a CPMG echo train with an echo time of 140 μs was measured. Up to a drying time of 4 h, 128 echoes were used in the CPMG train, the recycle delay was 1 s, and the number of scans 48, leading to a total experimental time of 18 min. Beyond 4 h, the number of echoes was changed to 64, the recycle delay to 0.7 s, and the number of scans to 128, so the total experimental time was 33 min. The amplitudes reported on the plots are the amplitudes obtained from a single exponential fit of the CPMG decay.

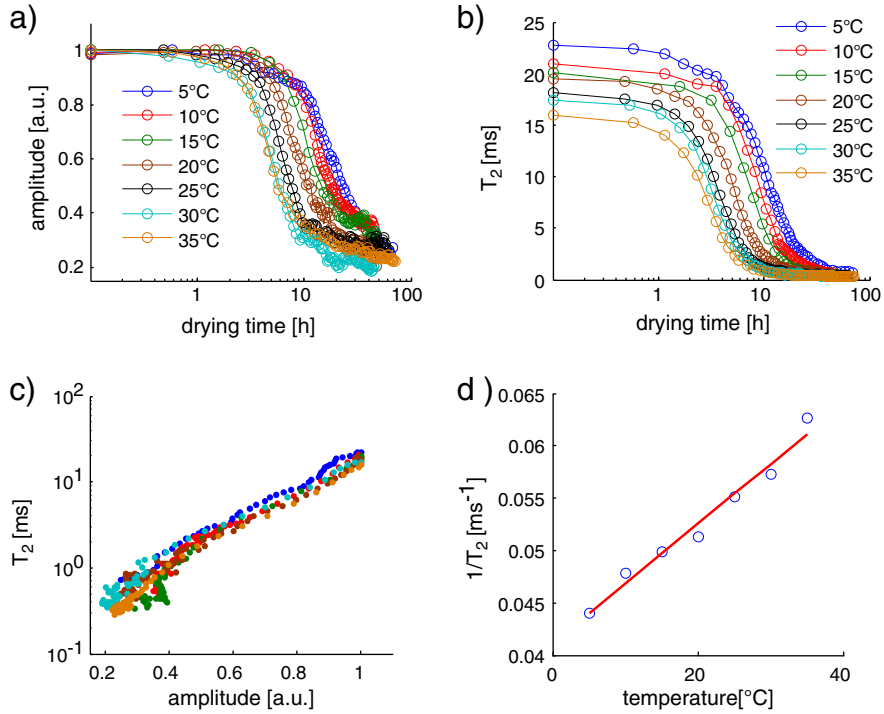

Fig. 8. Amplitudes and T_2 relaxation times as functions of the drying time measured with the Profile MOUSE at a depth of 10 mm from the surface in a sample of white cement (w/c = 0.4). For these measurements, a CPMG detection train with an echo time of 140 μs was employed. Up to a drying time of 4 h, 128 echoes were used in the CPMG train, the recycling delay was 1 s and the number of scans 256, leading to a total experimental time of 4 min. Beyond 4 h, the number of echoes was changed to 64, the recycle delay to 0.7 s, and the number of scans to 512, so the total experimental time was 6 min. The amplitudes and T_2s reported on the plots are obtained from single exponential fits of the CPMG decays. a) Evolution of the amplitude versus the hydration time at various temperatures. b) Evolution of T_2s versus the hydration time at various temperatures. c) Correlation between amplitudes and T_2s at various temperatures. d) Correlation between the relaxation rates measured at the initial drying time and temperature.

spherical pores. Thus, it sounds reasonable to find a power 3 law dependence of the apparent T_2 with the amplitude. This validates a posteriori the use of Eq. (1).

We showed that the Profile MOUSE is a very powerful tool which allows to observe simply the effect of drying and its consequence on the distribution of free water within the sample. In fact, it acts as a natural filter to exclusively observe the distribution of free water in white cement pastes. However, the disentanglement of drying and self-desiccation effects requires the use of the complementary STRAFI tool.

3.4. Effect of relative humidity on the drying profiles

At this stage, it can be argued that the NMR signal is not sensitive to the total amount of water. As we have seen before, C–H and hydroxyl groups in the C–S–H have very short T_2 values (a few tens of microseconds typically). If a part of the Portlandite NMR signal is missed, the observed total amount of water should decrease with the hydrating time, even without any evaporation effect. In order to check this and obtain an evaluation of the missing signal, the paste was hydrated in a confined environment so that no water was lost (experiment at 100%RH). The result is displayed in Fig. 9. In this figure, one can see that the green curve slightly decreases with time. This decrease corresponds to a loss of 15% of the initial amplitude in 20 h of hydration. This effect is attributed to the conversion of free water into chemically combined water (C–H and C–S–H) whose T_2 is too short to be recorded.

To follow the influence of the humidity level on the desiccation of white cement paste, STRAFI profiles were acquired along the hydrating time at 22 °C and relative humidity of 20%. For each position of the profile, the CPMG signal was fitted by a bi-exponential decay. The amplitude of both exponentials at two positions in the profile is displayed Fig. 10. The effect of the drying is clearly evidenced. In the bulk (Fig. 10a), the decrease of free water (red squares) mainly corresponds as expected to a conversion of free water into gel water. The setting of the cement paste was observed at the hydration time $t = 7$ h. Fig. 10b evidences a marked evaporation effect. Before a hydration time of 5 h, the free water (red squares) strongly decreased because of evaporation. As a consequence, after the setting time, the weak amount of remaining free water was converted into gel water, and the drying rate was slowed down. As a noteworthy result, the behavior obtained for the bulk is the same for all positions in the paste. This is clearly

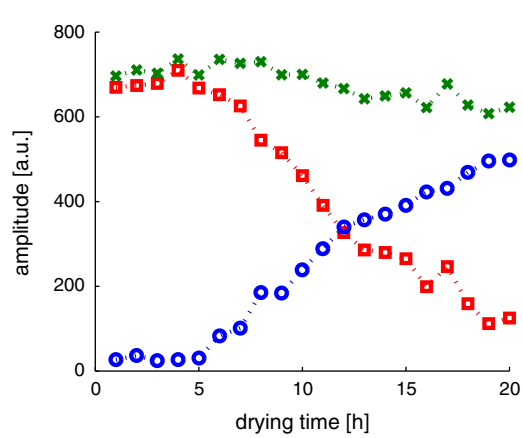

Fig. 9. Evolution of free (red squares) and "gel" (blue circles) water along the hydration time of a white cement paste (w/c = 0.4) at 22 °C and 100% RH. The observed slice was at a depth of 5 mm from the surface in the bulk. A CPMG detection train was performed with an echo time of 16 μs. The sum of both the free and the "gel" water is represented by the green line.

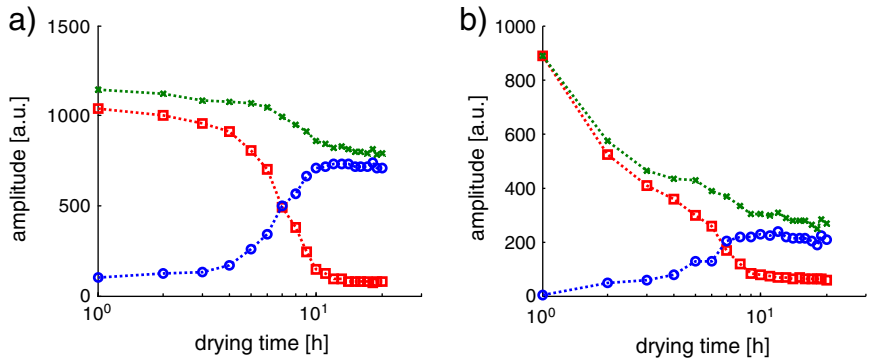

Fig. 10. Evolution of the weight of the long (red squares) and short (blue circles) T_2 components along the hydration time for two positions in a profile of a white cement paste (w/c = 0.4) obtained at 22 °C with a relative humidity of 20%. The green curve corresponds to the total recorded water signal in the sample (free and gel water). a) is obtained from a slice in the bulk of the paste, and b) is obtained at the surface (less than 1 mm from the surface).

consistent with the results obtained with the Profile MOUSE (Fig. 7): below 25 °C, the effect of the drying is effective up to a distance of 1 mm from the surface. For deeper positions in the paste, the water transport throughout the sample produced a homogeneous distribution of water in the paste. At this stage, it can be noticed that the total amount of free water in the bulk was slowly decreased. Indeed, it appears that before the setting of the paste, the bulk is slowly and homogeneously drying.

4. Conclusion

It is well known that the hydrating white cement paste develops a discrete porous network with a smallest pore diameter of 2.4 nm. For the first time, the discrete behavior of a hydrating cement paste has been spatially resolved. The combination of two complementary techniques (the MOUSE and the STRAFI techniques) provided the opportunity to disentangle evaporation from hydration for different conditions of temperatures and relative humidity. While the STRAFI technique can detect the gel water as well as the capillary water, the MOUSE technique acts as a filter for the capillary water. Both techniques have been used to study the drying of a hydrating cement paste cylinder with one surface in contact with air.

The analysis of the spatially resolved T_2 distribution gave the following results: The T_2 of the water in the capillary pores progressively decreased from a few ms to 400 μs. The $T_2 = 150$ μs of the gel water could be detected after 1 h and remained constant over time.

2D $T_1 - T_2$ localized experiments have been successfully performed at the beginning of the hydration and after 4 days of hydration. The $T_1 - T_2$ experiment allowed to validate the proton relaxation model in a STRAFI experiment. The 2D experiment gave the same T_2 distribution as in the simple STRAFI experiment. The discrete nature of the pore network was evidenced after 4 days.

Another conclusion could be drawn from the experiments at different temperatures. Below 25 °C the drying was homogeneous, the kinetics of structuring of the paste as well as the amount of water were the same whatever the position in the sample, except for a thin layer at the surface of the sample. The thickness of this layer varied with the drying time. It measured about 3 mm after 30 h of hydration. Above 25 °C, the water profile was no longer homogeneous: On the contrary, the occurrence of a gradient of water content was consistent with a transition from a funical behavior toward a pendular behavior. At this temperature, the pore network was too dense to allow efficient capillary water transfer.

Two situations have been compared to evidence the effect of relative humidity. In the first case, the hydration occurred under a relative humidity of 100% and in the second case, the relative humidity was 20%. A STRAFI experiment allowed to check that the loss of the water signal was due to the true drying process (capillary water evaporation) and not to the hydration (conversion of capillary water with "long" T_2 values into structural water of "short" T_2 values). The effect of the low relative humidity was to desaturate a layer at the surface of the drying sample. Elsewhere, the water distribution remained homogeneous.

References

[1] P. Coussot, Scaling approach of the convective drying of a porous medium, Eur. Phys. J. B. 15 (3) (2000) 557–566.
[2] P. Faure, P. Coussot, Drying of a model soil, Phys. Rev. E 82 (2010) 036303.
[3] H.F.W. Taylor, Cement Chemistry, Academic Press, 1990.
[4] F. Barberon, J.P. Korb, D. Petit, V. Morin, E. Bermejo, Probing the surface area of a cement-based material by nuclear magnetic relaxation dispersion, Phys. Rev. Lett. Chem. 90 (2003) 116103.
[5] J.R. Zimmerman, W.E. Brittin, NMR studies in multiple phase systems: lifetime of a water molecule in an adsorbing phase on silica gel, J. Phys. Chem. 61 (1957) 1328–1333.
[6] W.P. Halperin, J.-Y. Jehng, Y.Q. Song, Application of spin–spin relaxation to measurement of surface area and pore size distribution in a hydrating cement paste, Magn. Reson. Imaging 12 (1994) 169–173.
[7] L. Venkataramanan, Y.Q. Song, M.D. Hürlimann, Solving Fredholm integrals of the first kind with tensor product structure in 2 and 2.5 dimensions, IEEE Trans. Signal Process. 50 (2002) 1017–1026.
[8] P.J. McDonald, J.P. Korb, J. Mitchell, L. Monteilhet, Surface relaxation and chemical exchange in hydrating cement pastes: a two-dimensional NMR relaxation study, Phys. Rev. E 72 (2005) 011409.
[9] P.J. McDonald, V. Rodin, A. Valori, Characterisation of intra- and inter-C–S–H gel pore water in white cement based on an analysis of NMR signal amplitudes as a function of water content, Cem. Concr. Res. 40 (2010) 1656–1663.
[10] J. Greener, H. Peemoeller, C. Choi, R. Holly, E.J. Reardon, C.M. Hansson, M.M. Pintar, Monitoring of hydration of white cement paste with proton NMR spin–spin relaxation, J. Am. Ceram. Soc. 83 (2000) 623–627.
[11] T. Nunes, E.W. Randall, A.A. Samoilenko, P. Bodart, G. Feio, The hardening of Portland cement studied by ^{1}H NMR stray-field imaging, J. Phys. D: Appl. Phys. 29 (1996) 805–808.
[12] A.J. Bohris, U. Goerke, P.J. McDonald, M. Mulheron, B. Newling, B. Le Page, A broad line NMR and MRI study of water and water transport in Portland cement pastes, Magn. Reson. Imaging 16 (1998) 455–461.
[13] J. Boguszynska, M.C.A. Brown, P.J. McDonald, J. Mitchell, M. Mulheron, J. Tritt-Goc, D.A. Verganelakis, Magnetic resonance studies of cement based materials in inhomogeneous magnetic fields, Cem. Concr. Res. 35 (2005) 2033–2040.
[14] P.J. McDonald, Stray field magnetic resonance imaging, Prog. Nucl. Magn. Reson. Spectrosc. 30 (1997) 69–99.
[15] T. Nunes, Influence of grain size on the setting of Portland cement: a stray-field magnetic resonance imaging study, Mater. Sci. Forum 514–515 (2006) 1633–1637.
[16] P.J. McDonald, J. Mitchell, M. Mulheron, P.S. Aptaker, J.-P. Korb, L. Monteilhet, Two-dimensional correlation relaxometry studies of cement pastes performed using a new one-sided NMR magnet, Cem. Concr. Res. 37 (2007) 303–309.
[17] B. Blümich, J. Perlo, F. Casanova, Mobile single-sided NMR, Prog. Nucl. Magn. Reson. Spectrosc. 52 (2008) 197–269.
[18] M. Van Landeghem, B. Bresson, B. Blümich, J.-B. d'Espinose de Lacaillerie, Micrometer scale resolution of materials by stray-field magnetic resonance imaging, J. Magn. Reson. 211 (2011) 60–66.
[19] J. Perlo, F. Casanova, B. Blümich, Profiles with microscopic resolution by single-sided NMR, J. Magn. Reson. 176 (2005) 64–70.
[20] M.D. Hürlimann, D.D. Griffin, Spin dynamics of Carr–Purcell–Meiboom–Gill-like sequences in grossly inhomogeneous B_0 and B_1 fields and applications to NMR well logging, J. Magn. Reson. 143 (2000) 120–135.

[21] E.W. Randall, A.A. Samoilenko, T. Nunes, Simultaneous ^{1}H and ^{19}F stray-field imaging in solids and liquids, J. Magn. Reson. Ser. A 117 (1995) 317–319.
[22] In: F. Casanova, J. Perlo, B. Blümich (Eds.), Single-sided NMR, Springer, Berlin/Heidelberg, 2011.
[23] G. Goelman, M.G. Prammer, The CPMG pulse sequence in strong magnetic field gradients with application to oil-well logging, J. Magn. Reson. Ser. A 113 (1995) 11–18.
[24] M.D. Hürlimann, L. Burcaw, Y.-Q. Song, Quantitative characterization of food products by two-dimensional DT_2 and T_1T_2 distribution functions in a static gradient, J. Colloid Interface Sci. 297 (2006) 303–311.
[25] P.J. McDonald, J. Mitchell, M. Mulheron, L. Monteilhet, J.-P. Korb, Two-dimensional correlation relaxation studies of cement pastes, Magn. Reson. Imaging 25 (2007) 470–473.
[26] J.L. Markley, W.J. Horsley, M.P. Klein, Spin–lattice relaxation measurements in slowly relaxing complex spectra, J. Chem. Phys. 55 (1971) 3604–3605.
[27] Y.-Q. Song, L. Venkataramanan, M.D. Hürlimann, M. Flaum, P. Frulla, C. Straley, T_1–T_2 correlation spectra obtained using a fast two-dimensional Laplace inversion, J. Magn. Reson. 154 (2002) 261–268.
[28] C.J. Brinker, G.W. Scherer, Sol–Gel Science: The Physics and Chemistry of Sol–Gel Processing, Academic Press, London, 1990.
[29] R. Holly, E.J. Reardon, C.M. Hansson, H. Peemoeller, Proton spin–spin relaxation study of the effect of temperature on white cement hydration, J. Am. Ceram. Soc. 90 (2) (2007) 570–577.
[30] K.O. Kjellsen, R.J. Detwiler, Reaction kinetics of Portland cement mortars hydrated at different temperatures, Cem. Concr. Res. 22 (1992) 1101–1114.
[31] R. Kimmich, NMR: Tomography, Diffusometry, Relaxometry, Springer, Berlin/Heidelberg, 1997.